Competing multiple oxidation pathways shape atmospheric limonene-derived organonitrates simulated with updated explicit chemical mechanisms

Qinghao Guo[1], Haofei Zhang[2], Bo Long[3], Lehui Cui[1], Yiyang Sun[1], Hao Liu[1], Yaxin Liu[1], Yunting Xiao[1], Pingqing Fu[1] and Jialei Zhu[1,*]

1 Institute of Surface-Earth System Science, School of Earth System Science, Tianjin University, Tianjin, 300072, China;

2 Department of Chemistry, University of California, Riverside, California 92521, USA;

3 College of Materials Science and Engineering, Guizhou Minzu University, Guiyang 550025, China.

Correspondence to: Jialei Zhu, Email: zhujialei@tju.edu.cn

Abstract. Organonitrates (ON) are key components of secondary organic aerosols (SOA) with potential environmental and climate effects. However, ON formation from limonene, a major monoterpene with unique structure, and its sensitivity to oxidation pathways remain insufficiently explored due to the absence of models with explicit chemical mechanisms. This study advances the representation of limonene-derived ON formation by incorporating 90 gas-phase reactions and 39 intermediates across three oxidation pathways (O_3, OH, NO_3) into both a chemical box model and a global model. Box model sensitivity experiments revealed that competition among major oxidation pathways, coupled with the high yield of limonene-derived ON from O_3-initiated oxidation, leads to increased limonene-derived ON production when the O_3-initiated pathway is enhanced, whereas strengthening the OH- or NO_3-initiated pathways reduces ON formation. Compared to the box model, the global simulation exhibits stronger nonlinear responses and great spatiotemporal variability in limonene-derived ON formation across different oxidation pathways. This is primarily driven by the complex distribution of precursors and oxidants, as well as changing in dominate chemical pathways under various meteorological conditions. In the presence of the other two pathways, increasing the O_3- or NO_3-initiated oxidation pathway reduces the global limonene-derived ON burden by 19.9% and 17.3%, respectively, whereas enhancing the OH-initiated pathway increases it by 44.7%. limonene-derived ON chemistry developed in this study not only enhances the global model's ability to simulate ON formation evaluated through comparison with observations but also demonstrates an approach based on explicit chemical mechanisms that establishes a methodological framework for simulating the chemical formation processes of SOA.

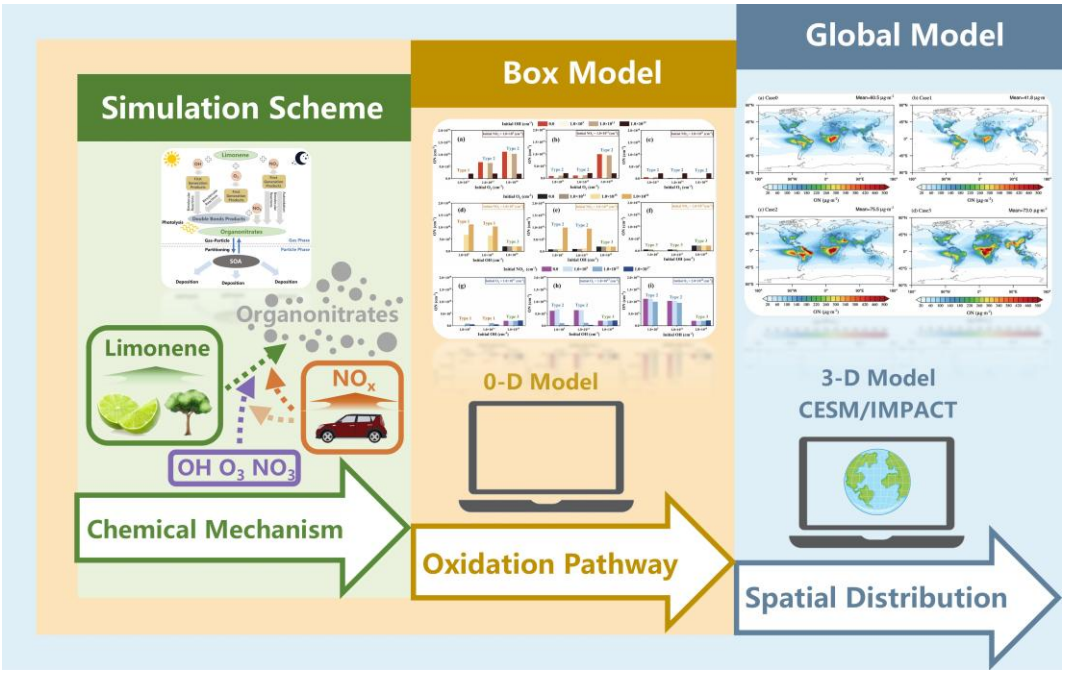

1 Introduction

Secondary organic aerosols (SOA) represent a substantial fraction of fine particulate matter and contribute to global public health risk, deterioration of air quality and climate change (Collaborators, 2024; Lelieveld et al., 2015; Tao et al., 2017). Among chemical constituents, organonitrates (ON) are of particular interest owing to their large fraction in SOA (5%-77%) (Farmer et al., 2010; Kiendler-Scharr et al., 2016). The rate of particulate ON formation contributes strongly to the rate of SOA formation at night, which emphasizes the important roles of particulate ON in ambient SOA (Guo et al., 2024). The nitrate group in ON would influence the physical and chemical properties of SOA, such as decreasing saturated vapor pressure of the product molecule (Capouet and Müller, 2006). ON are secondary compounds formed via the oxidation of volatile organic compounds (VOCs) in the presence of nitrogen oxides (NO_x = NO + NO_2), substantially influencing NO_x cycling and formation of ozone (O_3) and HONO (Perring et al., 2013). In global scale, VOCs are mainly emitted from biogenic sources, while NO_x are emitted from a wide variety of anthropogenic sources (Ng et al., 2017; Glasius and Goldstein, 2016). Therefore, a thorough investigation of ON is warranted to advance our understanding of interaction between biogenic and anthropogenic emissions.

The chemical formation mechanisms of ON are complex, hampering efforts to simulate and control SOA. In the daytime, hydroxyl radicals (OH) and ozone (O_3) oxidation of VOCs can produce peroxy

radical (RO_2), which reacts with NO_x to produce ON (Perring et al., 2013), while the reaction between nitrate radicals (NO_3) and VOCs dominates the generation of ON in the nighttime (Rollins et al., 2009; Perring et al., 2013; Ng et al., 2017). Furthermore, the coexistence among OH, O_3 and NO_3 has been investigated in VOCs nocturnal oxidation (Brown and Stutz, 2012; Barber et al., 2018; Kwan et al., 2012; Chen et al., 2022). Compared with single oxidant, the introduction of multiple oxidants leads to the possible complex reaction mechanisms for VOCs. The regeneration of OH would change the O_3 oxidation process to form SOA (Sato et al., 2013). Chamber experiments show that SOA from NO_3 oxidation of VOCs are affected by oxidation of NO_2 by O_3 (Ng et al., 2017). Therefore, VOCs are oxidized through the synergistic effects of multiple oxidants, driving the chemical formation of ON. However, ON formation from the VOCs oxidation governed by mixing oxidants has not been fully understood. In particular, the impact of oxidation pathways on the ON formation and spatial distribution are still unclear.

As one of typical biogenic volatile organic compounds (BVOCs) (10% of monoterpenes), limonene is mostly emitted from citrus plants and coniferous trees, with a total emission rate of ~11 $Tg \cdot yr^{-1}$ (Guenther et al., 2012; Sindelarova et al., 2014). Limonene has a unique structure with an endocyclic double bond and an exocyclic double bond, which makes it reactive towards atmospheric oxidants (Surratt et al., 2008). Higher ON (30–72%) and SOA yields (17–40%) through NO_3-initiated oxidation of limonene than other monoterpenes have been observed in laboratory experiments (Fry et al., 2014; Hallquist et al., 1999; Spittler et al., 2006; Moldanova and Ljungström, 2000; Fry et al., 2011). It has been well demonstrated that limonene + NO_3 is most important pathway to form limonene-derived ON (Kilgour et al., 2024; Ehn et al., 2014; Jokinen et al., 2015; Zhao et al., 2015). Furthermore, recent study found the primary nitrooxy RO_2 formed through NO_3 addition to limonene occurs at both at endocyclic double bond and the exocyclic double bond. These products could undergo autoxidation, which is fast enough to RO_2 bimolecular reactions (Mayorga et al., 2022). The molecular compositions and formation mechanism of limonene-derived ON have been well investigated through observations and laboratory studies, while their description in models remains not explicit and advanced.

The early atmospheric model utilizes empirical yields and empirical coefficients for predicting limonene-derived SOA production in simulation (Yu et al., 2019). Currently, chemical mechanisms are simplified according to analogies with structurally similar compounds in most of regional and global

models due to simplicity and efficiency in calculation (Fisher et al., 2016; Li et al., 2023a). Nevertheless, previous model studies have not included the formation mechanism of limonene-derived ON in detail (Pye et al., 2015; Li et al., 2023a; Zare et al., 2019). Thus, incorporating explicit mechanisms is helpful to understand limonene-derived ON formation process and the influence of interaction between multiple oxidation pathways on ON formation.

Herein, we investigated the impacts of multiple oxidation pathways on limonene-derived ON using both chemical box model and global model, which were developed to include explicit chemical mechanisms for limonene-derived ON formation. The effect of competition among individual oxidation pathways on limonene-derived ON formation were discussed using a chemical box model based on proposed mechanisms. The simulation framework of explicit chemical mechanisms was integrated into global model to evaluate the spatial distributions of limonene-derived ON and contributions of individual oxidation pathways. This study presents a numerical simulation framework for atmospheric chemical processes and aims at enhancing the ability of models to simulate ON and understand the competition effects among atmospheric oxidation pathways on SOA formation, improving atmospheric composition forecasts and informing interaction between biogenic and anthropogenic emissions.

2 Methodology

2.1 Limonene-derived ON formation mechanism

In order to simulate ON via the gas-phase oxidation of limonene, the chemical mechanism used in our model was updated with gas-phase chemical mechanisms of limonene-derived ON based on recent laboratory studies (Mayorga et al., 2022) and Master Chemical Mechanism (MCM, v3.3.1). The explicit chemical mechanism of limonene-derived ON involves three initial oxidation pathways: OH-, O_3- and NO_3-initiated oxidation (Fig. 1). The detailed formulas of species could be found in Table S1. The updated explicit formation mechanisms were list in Fig. S1 and Table S2. Compared to the MCM mechanism, the chemical mechanism of limonene-derived ON formation used in this study is developed to include: (1) NO_3 addition at three different carbonsites. Based on previous laboratory studies, the exocyclic double bond oxidation branching ratio is ~0.03 (Fry et al., 2011; Donahue et al., 2007), while the branching ratios of the two endocyclic $C_{10}H_{16}NO_5$-RO_2 isomers are 0.65:0.35

(Mayorga et al., 2022). Thus, these branching ratios of the three $C_{10}H_{16}NO_5$-RO_2 isomers were used in our work. (2) Sequential NO_3 oxidation reactions to form ON for all the products that contain double bonds from OH- and O_3-initiated oxidation in MCM. The rate constants were set to be the same as those used in MCM for limononaldehyde. (3) The formation of a ring-opened nitrooxy RO_2 in the presence of O_2 due to bond scission of the two endocyclic nitrooxy RO, and its branching ratio was estimated (Draper et al., 2019; Kurten et al., 2017; Guo et al., 2022). (4) H-shifts of the exocyclic $C_{10}H_{16}NO_4$-RO. (5) Bimolecular and unimolecular reactions of the $C_{10}H_{16}NO_6$-RO_2 and $C_{10}H_{16}NO_7$-RO_2. The rate constants for the bimolecular reactions are the same as those used in MCM, and autoxidation rate constants are calculated by quantum chemical calculations (Mayorga et al., 2022). In addition, photolysis, widely recognized as the predominant removal pathway of limonene-derived ON (Picquet-Varrault et al., 2020; Wang et al., 2023), is included in our mechanism. While heterogeneous processes and hydrolysis of limonene-derived ON are not included in our model, potentially resulting in a slight overestimation of simulated limonene-derived ON concentrations, their contributions to ON removal are expected to be substantially smaller than that of photolysis. Consequently, this omission introduces only minor uncertainties in our results. In our explicit chemical mechanism, more intermediates and chemical processes of limonene-derived ON were distinguished than simplified mechanisms used in previous models.

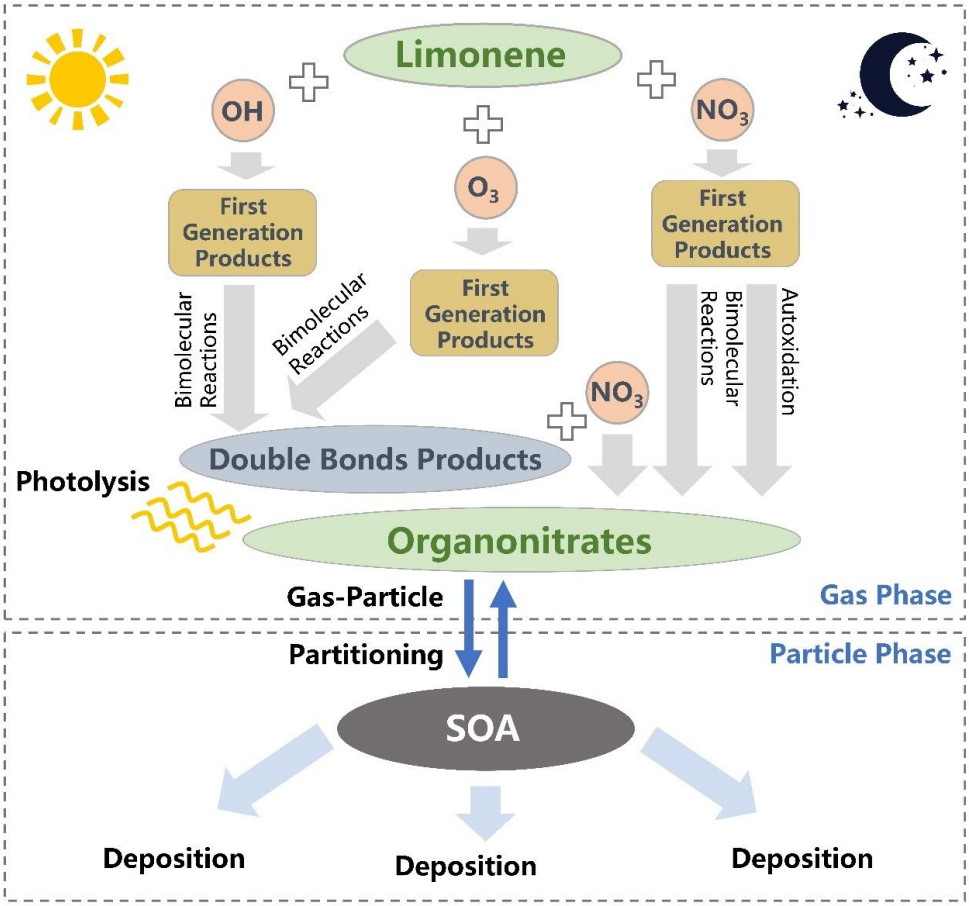

Figure 1. Schematic diagram of the limonene-derived ON formation pathways included in this work.

We assumed highly oxidated ON products ($C_{10}H_{13}NO_7$, $C_{10}H_{15}NO_4$, $C_{10}H_{15}NO_5$, $C_{10}H_{15}NO_6$, $C_{10}H_{15}NO_7$, $C_{10}H_{15}NO_8$, $C_{10}H_{17}NO_5$, $C_{10}H_{17}NO_6$, $C_{10}H_{17}NO_7$) to be semi- to low-volatile which can condense into the particulate phase upon formation. Their vapor pressures are estimated to calculate gas-particle partitioning (Table S3).

The vapor pressures of the above-mentioned ON species were estimated using two group contribution methods: EVAPORATION (Compernolle et al., 2011) and SIMPOL (Pankow and Asher, 2008). They are both widely used structure activity relationship (SAR)-based group contribution models to predict molecular vapor pressures. The key difference is that EVAPORATION considers proximity-based functional group interactions, so it considers differences in the locations of functional groups, while predictions from SIMPOL do not vary based on functional group locations. As a result, isomeric compounds with the same functional groups but different structures may have different predicted vapor pressures using EVAPORATION but the same using SIMPOL. Therefore, the

EVAPORATION model is preferred when chemicals structures are known while the SIMPOL model could be biased. In a recent study, we showed that the EVAPORATION-based kinetic model predicts isoprene SOA more accurately than the SIMPOL-based model, which underpredicts by ~ 20% (Shen et al., 2024).

In this work, because the chemical structures of the major ON species are known based on our recent work (Mayorga et al., 2022), we adopted the EVAPORATION method in all our simulations. As the EVAPORATION model input, the structures of the ON species from Mayorga et al. (2022) were converted to SMILES strings. To illustrate the difference between the two models, the EVAPORATION-predicted vapor pressures were compared with SIMPOL predictions (Table S3). The two methods predict vapor pressures within one order of magnitude in most cases, which is typically considered acceptable uncertainties for group contribution vapor pressure estimations.

2.2 Chemical box model

A zero-dimensional (0-D) chemical box model was used to examine the chemical processes of limonene-derived ON, investigating the contributions of atmospheric oxidants and oxidant pathways. The chemical mechanism presented in Fig. S1 and Table S2 was applied in this box model. To calculate the total production of limonene-derived ON, processes such as photolysis, dilution, and deposition were ignored for all chemical species in the model. The temperature was set to 298 K in the model. The initial concentrations of limonene and other atmospheric components for all cases were set as shown in Table S5. Limonene at a concentration of 1.0×10^{11} molecules·cm^{-3} was used as the precursor for ON, which falls within the range of values reported in laboratory and observation studies (Guo et al., 2022; Luo et al., 2023; Ham et al., 2016). The initial concentration of OH, O_3 and NO_3 spanned 1.0×10^{5} to 1.0×10^{19} molecules·cm^{-3}, 1.0×10^{11} to 1.0×10^{18} molecules·cm^{-3} and 1.0×10^{9} to 1.0×10^{17} molecules·cm^{-3}, respectively. The low values represent typical atmospheric concentrations of these species, which are within the range of those reported in previous studies (Shen et al., 2021; Liu et al., 2023; Matsunaga and Ziemann, 2019). The medium to high values represent extreme conditions, in order to investigate the significant impact of oxidants on limonene-derived ON across a broad spectrum of oxidant levels. Chamber experiments were simulated by the box model under ideal situation, which has been specifically design to analyze chemical processes, while simulations under real atmospheric

condition were carried using global model in sect. 2.3. We conducted sensitivity tests (Sect. S1 in the supplement) to examine oxidation pathways for formation of limonene-derived ON. Sensitivity tests under single initial oxidation were set. Building upon this foundation, sensitivity tests with multiple oxidation pathways were implemented: (1) introducing secondary oxidant across three concentration gradients under fixed primary oxidant levels, followed by (2) increasing concentration of third oxidant with three concentration gradients. A summary of all cases can be found in Table S4.

2.3 Simulation of global limonene-derived ON

We used the Community Earth System Model (CESM) version 1.2.2.1 coupled with the University of Michigan Integrated Massively Parallel Atmospheric Chemical Transport (IMPACT) aerosol model with a resolution of 1.9° × 2.5° for this study. The CESM/IMPACT model have included a fully explicit gas-phase photochemical mechanism to predict the formation of semi-volatile organic compounds (SVOCs) which then partition to an aerosol phase (Lin et al., 2014), facilitating the incorporation of explicit limonene-derived ON mechanism to simulate their global burden. The IMPACT aerosol module gets the meteorology field from the CESM model at each time step, while changes in the aerosols in IMPACT do not provide feedback to the CESM. The emission of precursors BVOCs are estimated by the Model of Emissions of Gases and Aerosols from Nature inventory (MEGAN) coupled to CESM/IMPACT model. The developed explicit gas phase chemical mechanism same as used in above chemical box model was applied to simulate the formation of limonene-derived ON. The highly oxidated limonene-derived ON considered as semi-volatile species partitioning from gas phase to particle phase contributes to SOA. A base case (Case0) was designed to simulate limonene-derived ON under all three initial oxidation pathways, and six sensitivity experiments were designed for simulating global burden limonene-derived ON under two initial oxidation pathways (Case 1-3) and single initial oxidation pathway (Case 4-6), respectively. Above seven cases were summarized in Supplementary Sect. S2 and Table S6.

3 Results and discussion

3.1 Limonene-derived ON formation through individual initial oxidation pathway.

We employed a chemical box model to simulate limonene-derived ON formed through three initial oxidation pathways, considering various oxidant concentrations (Fig. 2). These simulations were designed to evaluate the effect of increasing oxidant concentrations on the yield of limonene-derived ON from each initial oxidation pathway. In the case with individual OH oxidation pathway, the concentration of limonene-derived ON increases as the initial OH concentration increases (Fig. 2a), following a pattern to that of limonene consumption (Fig. S2a). Initial OH concentration increases from 1.0×10^{5} to 1.0×10^{19} molecules·cm^{-3}, resulting in ~20.0-fold increase in the production of limonene-derived ON. At this stage, limonene is not completely consumed by OH, indicating that higher initial OH concentration will increase consumption of limonene to produce more ON.

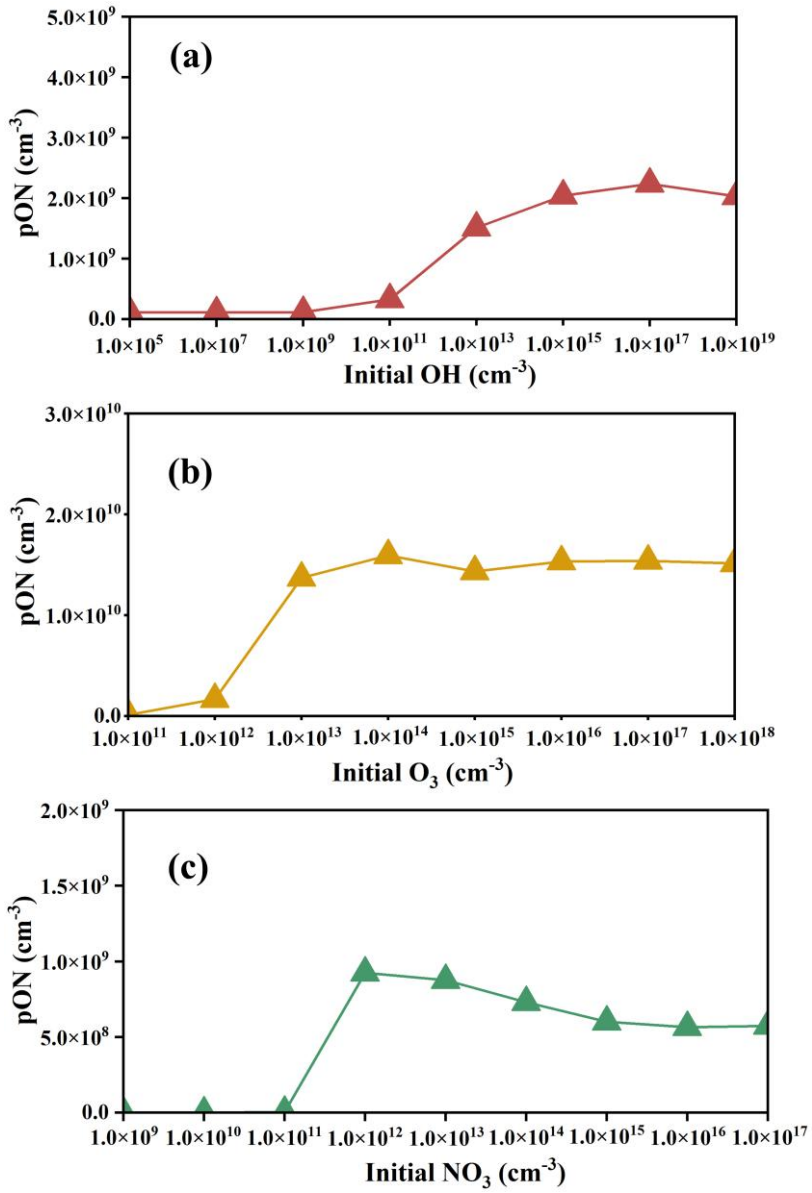

Figure 2. Variations of limonene-derived ON in individual oxidation pathway under different oxidant concentrations. The triangles represent concentration of limonene-derived ON in each experiment. The lines represent the trend of limonene-derived ON. The three datapoint colors represent three initial oxidation pathways (red for OH-initiated oxidation, yellow for O_3-initiated oxidation, green for NO_3-initiated oxidation).

In the case with individual O_3 oxidation pathway, the limonene-derived ON increases first and then maintains a relatively stable production with the increase of initial O_3 concentration (Fig. 2b). Limonene is not completely consumed when initial O_3 concentrations below 1.0×10^{14} molecules·cm^{-3}. Increased consumption of limonene lead to an increase in ON production with increased O_3 concentration.

Same to the cases of the OH- and O_3-initiated oxidation pathways, limonene-derived ON increases when initial NO_3 concentrations below 1.0×10^{12} molecules·cm^{-3} could be caused by incompletely consumed limonene (Fig. 2c). The increased consumption of limonene with increase in concentrations of NO_3 lead to the increased production of ON. However, different from the cases of OH- and O_3-initiated oxidation pathways, as initial NO_3 concentrations continued to increase, limonene-derived ON production decrease. When limonene-derived ON concentrations reached steady state within 30 minutes, compared to the case with initial NO_3 concentration of 1.0×10^{12} molecules cm^{-3}, reaction of LIMAL and NO_3 become the dominant pathway in the case with initial NO_3 concentration of 1.0×10^{17} molecules·cm^{-3}. The lower yield of the NO_3 oxidation pathway (9.2%) of LIMAL relative to OH oxidation pathway (28.8%) results in decreased limonene-derived ON (green box in Fig. S1). The results mean that at low initial oxidant concentration, limonene-derived ON shows a strong dependence on initial oxidant concentration, and the dependence on intermediate reaction rates becomes more important at high initial oxidant concentration.

In addition, average concentration of ON of OH-, O_3- and NO_3-initiated oxidation pathways when oxidations are sufficient are calculated separately. The O_3-initiated oxidation pathway (1.5×10^{10} molecules·cm^{-3} limonene-derived ON produced) yields more ON than the OH- (2.1×10^{9} molecules·cm^{-3} limonene-derived ON produced) and NO_3-initiated (7.1×10^{8} molecules·cm^{-3} limonene-derived ON produced) oxidation pathways when limonene initial concentration is constant. This indicates that under initial conditions with sufficient oxidation, O_3-initiated oxidation pathway of limonene has highest yield of ON, which is about 15.0%, while that is low by OH- (2.1%) and NO_3-initiated (0.7%) oxidation pathway. This difference in the ON yield among various oxidation pathways will be used to explain the contributions of each oxidation pathway to ON concentration in the following discussion.

3.2 Effects of multiple oxidation pathways on limonene-derived ON formation.

Compared to the simulation scheme with individual oxidation pathway discussed above, introducing multiple oxidation pathways leads to comprehensive competition among them, which results in a nonlinear response of ON concentration to changes in the initial concentrations of oxidants. Figure 3 shows the dependence of limonene-derived ON on initial concentration of oxidants when include two initial oxidation pathways. The addition of oxidants has various effects on the yield of limonene-

derived ON. When the initial concentration of oxidant is low (1.0×10^5 molecules·cm^{-3} for OH, 1.0×10^{11} molecules·cm^{-3} for O_3, 1.0×10^9 molecules·cm^{-3} for NO_3), the initial limonene will not be completely consumed. In all case with low concentration of oxidants, adding another oxidant with oxidation pathway will increase consumption of limonene, leading to increase in the limonene-derived ON production. When the initial concentration of oxidants is high, limonene will be nearly or completely consumed. In these cases, the production of limonene-derived ON will be determined by the competition between the two oxidation pathways. The product of limonene-derived ON steadily increased as the initial concentration of O_3 increases from 0 to 1.0×10^{18} molecules·cm^{-3} when the initial concentration of OH or NO_3 is constant (Fig. 3a, f). According to the chemical mechanism applied in the model, the reaction between limonene and O_3 has higher rate than OH and NO_3 in these cases (Table S7). As a result, in the presence of O_3, the oxidation of limonene with O_3 proceeds more rapidly than with OH or NO_3, leading to higher concentration of limonene-derived ON due to the high yield of O_3 oxidation pathway as discussed in above section (compare Fig. 2b with Fig. 2a and 2c). In contrast, compared to only including O_3 oxidation pathway, adding oxidation pathways with OH or NO_3 will result in a decrease in limonene-derived ON production (Fig. 3c, d), because some limonene that would have reacted with O_3 is instead converted to ON through the OH or NO_3 pathways with lower yield. Therefore, the dominant oxidation pathway and its ON yield determine the impact of the competition between the two oxidation pathways on the final limonene-derived ON production. A similar phenomenon observed in laboratory study shows that NO_x influences γ-terpinene ozonolysis by enhancing NO_3 production at high NO_x levels, which subsequently leads to NO_3 preferentially consuming γ-terpinene over O_3 (Xu et al., 2020), illustrating the competition between oxidants. The addition of the OH-initiated oxidation pathway results in a small increase in ON production compared to NO_3-initiated oxidation alone (Fig. 3e), due to the slightly higher yields of limonene-derived ON for OH-initiated oxidation pathway. The ON production would not change much when add the NO_3-initiated oxidation pathway compared to the case with OH-initiated oxidation pathway alone (Fig. 3b) because of unchanged the main initial oxidation pathway. These sensitivity experiments suggest that competition of oxidation pathways plays an important role in formation of limonene-derived ON.

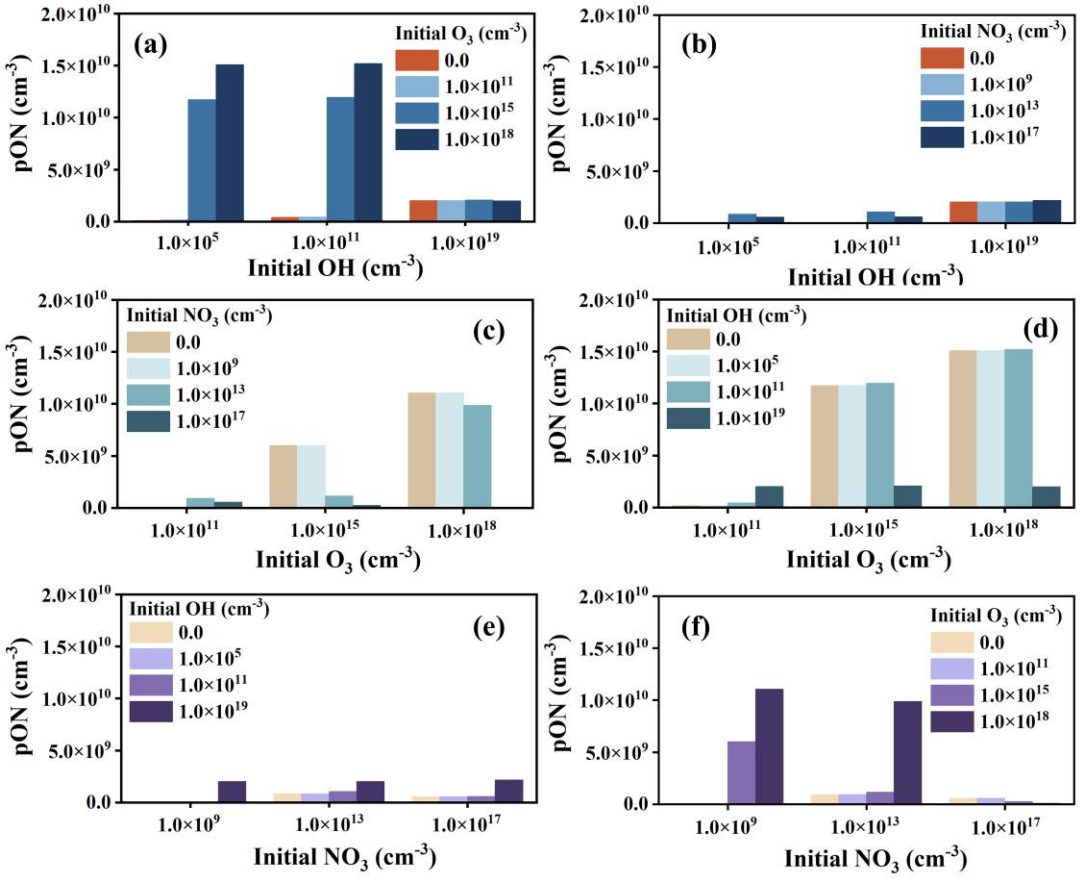

Figure 3. Simulated limonene-derived ON in two initial oxidation pathways under different oxidant conditions, including variation of production of limonene-derived ON with adding (a) initial O_3 concentration and (b) initial NO_3 concentration in the three OH levels; variation of limonene-derived ON production with adding (c) initial OH concentration and (d) initial NO_3 concentration in the three O_3 levels; variation of limonene-derived ON production with adding (e) initial OH concentration and (f) initial O_3 concentration in the three NO_3 levels.

Based on the production variations of limonene-derived ON in the cases with one and two initial oxidation pathways discussed above, the comprehensive impact of multiple oxidants on limonene-derived ON formation in the cases with multiple initial oxidation pathways are analyzed (Fig. 4). The results can be summarized into three types. The Type 1 is the cases when limonene is not completely consumed (Fig. S4). When two initial oxidant concentration is low (Fig. 4a, d, g) and medium (Fig. 4d, g), the addition of third oxidant increases the production of limonene-derived ON because the addition of the third oxidant increases consumption of limonene. If the oxidant concentration is sufficient to consume up limonene, the production of limonene-derived ON will be determined by the competition between initial oxidation pathways. The Type 2 is the cases with large changes of limonene-derived ON. Under low NO_3 and moderate and high O_3 conditions, the production of limonene-derived ON decreases with adding OH (Fig. 4a, b), because some limonene that would have reacted with O_3 is

instead converted to ON through the OH pathways with lower yield. The formation of limonene-derived ON shows similar pattern for Type 2 in Figure 4h and i. On the one hand, the yield of limonene-derived ON from NO_3-initiated oxidation is lowest, so the production of limonene-derived ON will decrease when the formation of limonene-derived ON from this pathway becomes the dominant formation route. On the other hand, adding NO_3-initiated oxidation pathway also consumes NO_3 that would have reacted with the product of the OH- and O_3-initiated oxidation, resulting in decrease production of limonene-derived ON. The changes in ON production with constant initial concentration of limonene and various oxidation pathways indicate the interactions of different oxidation process of limonene. In contrast to OH- and NO_3-initiated oxidation pathway, adding oxidation pathways with O_3 will result in increase in limonene-derived ON production (Fig. 4e), due to higher yield of limonene-derived ON from O_3-initated oxidation pathway than OH- and NO_3-initated oxidation pathways. Since the yield of limonene-derived ON of OH-initiated oxidation is higher than NO_3-initiated oxidation, the production of limonene-derived ON decreases (Fig. 4c) as the main oxidation pathway changes from NO_3 to OH oxidation (Table S8). Additionally, in some sensitivity experiments (Fig. 4d-i), ON concentration do not change much with the addition of an oxidation pathway (Type 3). This could be explained by minimal competition with the rapid main oxidation pathway. These sensitivity experiments suggest that the limonene-derived ON production in the simulated system are not only controlled by limonene concentration, but also affected by synergic effect of multiple oxidants and oxidation pathways.

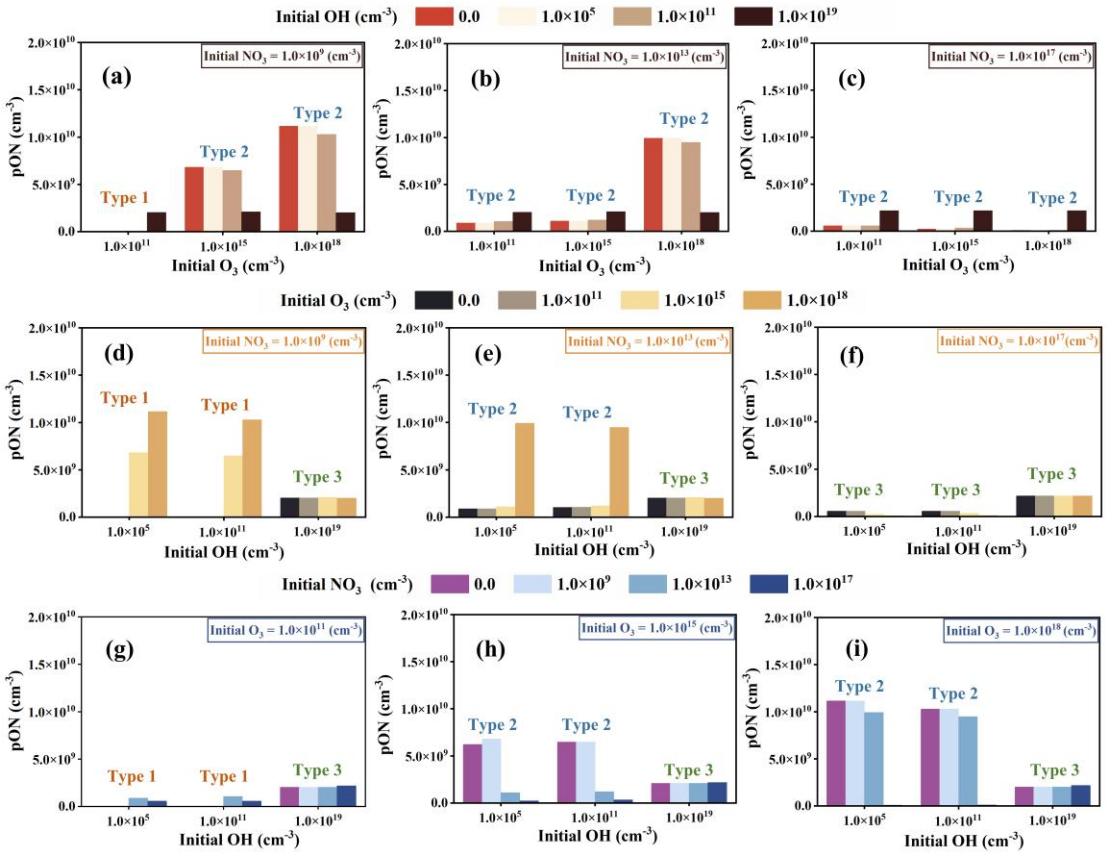

Figure 4. The influence of adding OH-, O_3- and NO_3-initiated oxidation pathways on the production of limonene-derived ON under different oxidant conditions, including variation of limonene-derived ON production with adding initial OH concentration in the three O_3 levels under (a) low, (b) moderate and (c) high NO_3 levels; variation of limonene-derived ON production with adding initial O_3 concentration in the three OH levels under (d) low, (e) moderate and (f) high NO_3 levels; variation of limonene-derived ON production with adding initial NO_3 concentration in the three OH levels under (d) low, (e) moderate and (f) high O_3 levels. In each panel, the types marked on the columns show the cases when limonene is not completely consumed (type 1) and almost completely consumed (large (type 2) and small (type 3) changes in limonene-derived ON production).

3.3 Contribution of each oxidation pathway to global limonene-derived ON.

Global simulation using CESM/IMPACT model was performed to characterize the spatial and temporal distribution of limonene-derived ON and the contributions of each oxidation pathway to global burden. Incorporation of formation of limonene-derived ON reduces underestimation of simulated ON by comparison with observations summarized in the literature (Sect. S3 in the supplement) (Li et al., 2023b). The spatial distribution of limonene-derived ON is shown in Fig. 5a. The simulated global mean limonene-derived ON burden is about 60.5 $\mu g \cdot m^{-2}$, and the highest burdens (>500 $\mu g \cdot m^{-2}$) are predicted over tropical forest regions of central Africa. As the primary precursor of limonene-derived ON, the concentration of limonene dominates the yield of these ON compounds. The seasonal cycle of simulated limonene-derived ON is presented in Fig. S6, which is mainly depend on

limonene levels. Global average limonene-derived ON burden peaks in the summer (69.2 $\mu g \cdot m^{-2}$) due to highest global average limonene concentration (Fig. S7b), while the large burden of limonene-derived ON in fall is driven by the presence of both high limonene concentration (Fig. S7c) and NO concentration (Fig. S8c) compared to spring and winter. In contrast, the burden of limonene-derived ON is lowest in winter (48.1 $\mu g \cdot m^{-2}$) because of lowest concentration of limonene (Fig. S7d). Beyond the effects of limonene and NO concentrations, oxidant levels and oxidation pathways also affect the formation mechanisms and production of limonene-derived ON, which may explain the highest burden in regions such as Central Africa, rather than Amazon where limonene concentrations are highest over the world (Fig. S9a). The concentration of oxidants is inherently low in Amazon (Fig. S9b-d) and oxidant scavenging in the presence of isoprene with high concentrations greatly reduce the photochemical formation of limonene-derived ON (Mcfiggans et al., 2019). Thus, oxidant competition with isoprene leads to low burden of limonene-derived ON in Amazon despite the highest burden of limonene there. Therefore, high concentrations of limonene-derived ON can only form when both high limonene and oxidant concentrations are present simultaneously.

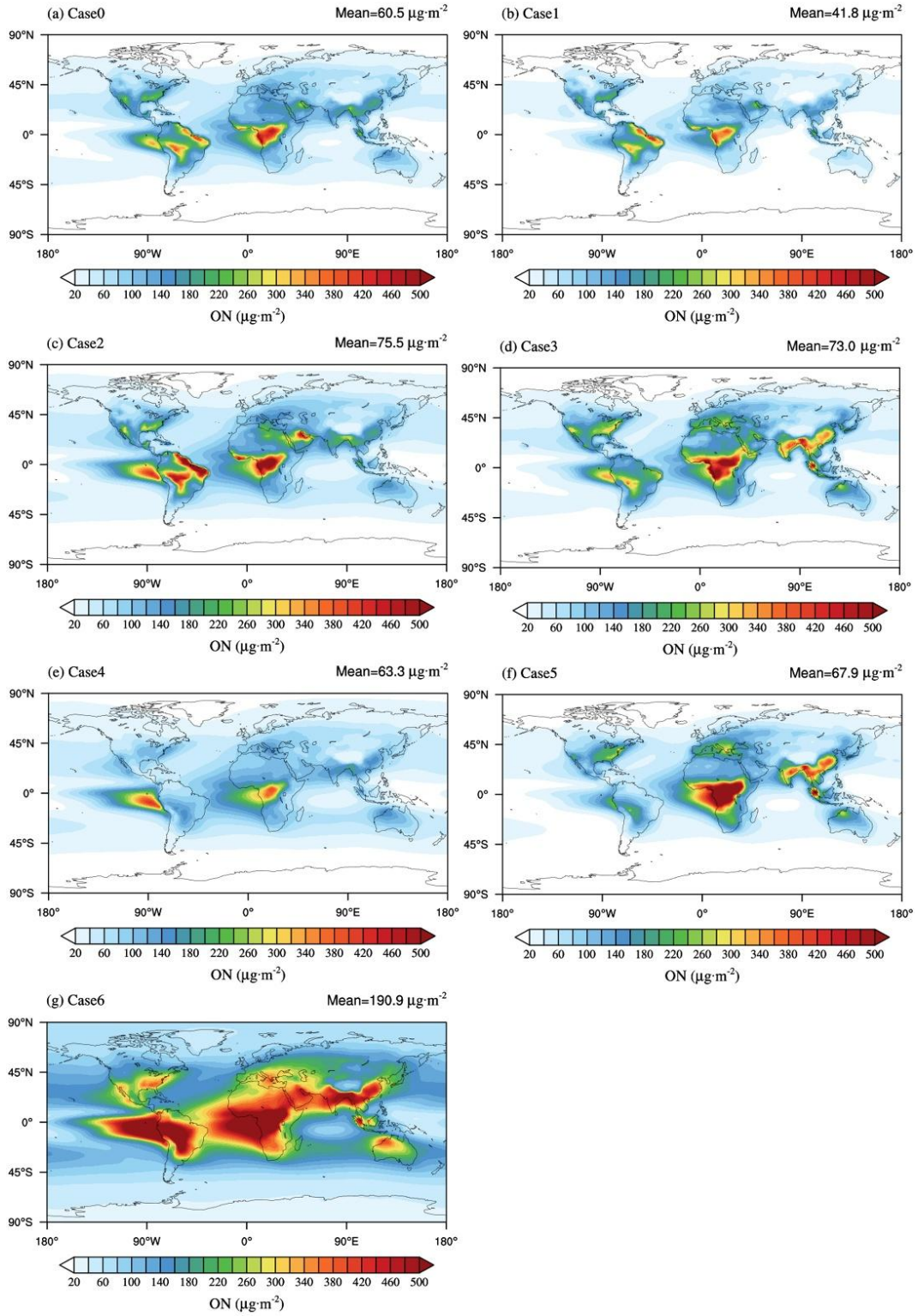

Figure 5. Annual mean column concentration of limonene-derived ON with different simulation schemes. (a) Run with three initial oxidation pathways (Case0), (b) without OH-initiated oxidation pathway (Case1), (c) without O_3-initiated oxidation pathway (Case2), (d) without NO_3-initiated oxidation pathway (Case3), (e) without O_3- and NO_3-initiated oxidation pathways (Case4), (f) without OH- and NO_3-initiated oxidation pathways (Case5) and (g) without OH- and O_3-initiated oxidation pathway (Case6).

To quantify the contribution of each oxidation pathway to the formation of limonene-derived ON in different regions, we conducted a series of sensitivity experiments (Case1 to 6 introduced in method section) on the oxidation pathways (Fig. 5b-g). Our simulations indicate that increasing O_3 and NO_3-initiated oxidation pathways result in 15.5% and 18.0% increase of global average burden of limonene-derived ON, respectively, compared to OH-initiated oxidation pathway alone (Fig. S10a, b). This is primarily because higher yields of limonene-derived ON associated with the O_3- and NO_3-initiated oxidation pathways compared to OH-initiated oxidation pathways. When compared to O_3-initiated oxidation pathway alone (Fig. S10c, d), the addition of OH- or NO_3-initiated pathways result in increased burden of limonene-derived ON in the limonene-sufficient region (e.g. Amazon), owing to adding a limonene-derived ON formation pathway to consume more limonene. However, in the limonene-deficient yet NO_3-sufficient regions (e.g. Central Africa, Mediterranean, and middle and low latitude of Asia), increasing the OH- or NO_3-initiated oxidation pathways reduces the burden of limonene-derived ON. This occurs because the oxidation of limonene by OH or NO_3 suppresses O_3-initiated oxidation, which otherwise produces limonene-derived ON with a high yield. Additionally, if limonene undergoes oxidation by NO_3, the availability of NO_3 for the nitration of OH- and O_3-initiated oxidation products of limonene will decrease, resulting in a reduction in limonene-derived ON. The addition of OH- and O_3-initiated oxidation pathways reduces global average burden of limonene-derived ON by 60.5% and 78.1% respectively, compared to the case with NO_3-initiated oxidation pathway alone (Fig. S10e, f). This reduction is likely due to insufficient NO_3 oxidation at night to further oxidize intermediates produced from OH- and O_3-initiated limonene oxidation during the day, limiting the formation of limonene-derived ON at night.

The burden of limonene-derived ON undergoes a noticeable change when an additional oxidation pathway is introduced to the existing two pathways (Fig. S11). Adding OH-initiated oxidation pathway increases the global average burden of limonene-derived ON from 41.8 to 60.5 $\mu g \cdot m^{-2}$, by 44.7%, while adding O_3-initiated oxidation pathway decrease that from 75.5 to 60.5 $\mu g \cdot m^{-2}$, by 19.9% (Fig. S11a, b), which was attributed to the competition between the OH and O_3 oxidation pathways for reactions with limonene. Compared to the simplified condition in simulation using chemical box model, global simulation considers diurnal variations of oxidation. When the O_3-initiated oxidation pathway produces the same amount of limonene-derived ON as the OH-initiated pathway, it consumes more

NO_3. As a result, increasing the O_3 oxidation pathway reduces the availability of NO_3 for the nitration of intermediate oxidation products in the nighttime, thereby lowering the total limonene-derived ON yield across all three pathways. In contrast, enhancing the OH oxidation pathway increases the total yield. Moreover, the addition of the NO_3-initiated oxidation pathway increases burden of limonene-derived ON in the limonene-sufficient region even over 150 $\mu g \cdot m^{-2}$ (Fig. S11c). However, in the region with high NO_3 concentration, the burden of limonene-derived ON decreases (Fig. S11c) because the NO_3-initiated oxidation pathway yields less limonene-derived ON than the O_3- and OH-initiated oxidation pathways. These results highlight the different nonlinear responses of limonene-derived ON to multiple oxidation pathways under varying oxidation conditions and precursor concentrations. This discrepancy highlights differences between global-scale dynamics and idealized box model conditions, emphasizing the importance of developing explicit chemical mechanisms in global models for understanding SOA formation processes. Prior laboratory study has also demonstrated that investigating the response of ON reveals complex and nonlinear behaviour with implications that could inform expectations of changes to ON concentrations as efforts are made to reduce oxidant concentrations (Mayhew et al., 2023).

4 Conclusion and implications

In this work, the explicit chemical mechanism is developed to simulate formation and spatial distribution of limonene-derived ON using a chemical box model and global model CESM/IMPACT. Under multiple initial oxidation pathways, limonene-derived ON shows non-linear variations with different oxidant conditions, which is controlled by the synergetic effects of multiple oxidants. When limonene is not consumed, adding another oxidant with oxidation pathway will increase limonene-derived ON due to increased consumption of limonene. When limonene is completely consumed, limonene-derived ON production is dominated by competition of oxidation pathways. The production of limonene-derived ON is increased by O_3-initiated oxidation pathway while decreased by OH and NO_3-initiated oxidation pathway. This is mainly because limonene oxidated by O_3 produces more ON than OH and NO_3, resulting from the simulation under individual initial oxidation pathway.

The global model simulation indicates that oxidation process is important for limonene-derived ON formation in addition to limonene concentration. Global limonene-derived ON burden decreases by

19.9% and 17.3% due to O_3- and NO_3-initiated oxidation pathway, while OH-initiated oxidation pathway increases global limonene-derived ON burden by 44.7% compared the case only including the other two oxidation pathways. These differences can be attributed to the complex nonlinear response of limonene-derived ON yield to different reaction pathways under varying precursor and oxidant conditions.

The chemical mechanism of ON formation may influence the formation and spatial distribution of ON. We only include main oxidation process published to date in the model, while some pathways (i.e. Heterogeneous NO_3 reactions) of ON is missing in this work. Gas-phase oxidation in our mechanism is considered as the dominant formation pathway of ON (Fan et al., 2022; Perring et al., 2013). Future inclusion of newly identified and quantified ON chemistry may lead to unpredictable nonlinear impacts on simulation outcomes. Although uncertainties remain in simulating limonene-derived ON due to limited knowledge of its formation mechanism, this work offers an improvement in the global model's ability to simulate ON and presents a methodological framework for simulating SOA and their chemical processes. This framework can be used in the future to improve SOA burden predictions and provide a comprehensive understanding of the complex interactions between multiple oxidation pathways, which are crucial for SOA formation (Chen et al., 2022; Zang et al., 2024). Quantitative understanding of these complex interactions in contributing to SOA formation can definitely facilitate better understanding the contributions of interactions and antagonistic actions between anthropogenic and natural emissions to atmospheric aerosols. These works provide valuable insights for making more effective secondary aerosol pollution control strategies to improve air quality.

Data availability. Simulation data are available upon request to the corresponding authors.

Author contributions. QG and JZ designed the study, developed the chemical box model and global model conducted the simulations, analyzed the data, and wrote the manuscript. HZ and BL provided the laboratory data. PF, LC, YS, HL, YL and YX contributed to the discussion and revision of the paper.

Competing interests. The authors declare no competing financial interest.

Disclaimer. Publisher's note: Copernicus Publications remains neutral with regard to jurisdictional claims in published maps and institutional affiliations.

Acknowledgments. The authors acknowledge the financial support of the National Natural Science Foundation of China.

Financial support. This study was supported by the National Natural Science Foundation of China (Grant 42177082).

References

Barber, V. P., Pandit, S., Green, A. M., Trongsiriwat, N., Walsh, P. J., Klippenstein, S. J., and Lester, M. I.: Four-Carbon Criegee Intermediate from Isoprene Ozonolysis: Methyl Vinyl Ketone Oxide Synthesis, Infrared Spectrum, and OH Production, J. Am. Chem. Soc., 140, 10866-10880, https://doi.org/10.1021/jacs.8b06010, 2018.

Brown, S. S. and Stutz, J.: Nighttime Radical Observations and Chemistry, Chem Soc Rev, 41, 6405-6447, https://doi.org/10.1039/c2cs35181a, 2012.

Capouet, M. and Müller, J. F.: A Group Contribution Method for Estimating the Vapour Pressures of α-pinene Oxidation Products, Atmos. Chem. Phys., 6, 1455-1467, https://doi.org/10.5194/acp-6-1455-2006, 2006.

Chen, Y., Tan, Y., Zheng, P., Wang, Z., Zou, Z., Ho, K. F., Lee, S., and Wang, T.: Effect of NO_2 on Nocturnal Chemistry of Isoprene: Gaseous Oxygenated Products and Secondary Organic Aerosol Formation, Sci. Total Environ., 842, 156908, https://doi.org/10.1016/j.scitotenv.2022.156908, 2022.

Collaborators, G. B. D. R. F.: Global burden and strength of evidence for 88 risk factors in 204 countries and 811 subnational locations, 1990-2021: a systematic analysis for the global burden of disease study 2021, Lancet, 403, 2162-2203, https://doi.org/10.1016/S0140-6736(24)00933-4, 2024.

Compernolle, S., Ceulemans, K., and Müller, J. F.: EVAPORATION: a new vapour pressure estimation methodfor organic molecules including non-additivity and intramolecular interactions, Atmos. Chem. Phys., 11, 9431-9450, https://doi.org/10.5194/acp-11-9431-2011, 2011.

Donahue, N. M., Tischuk, J. E., Marquis, B. J., and Huff Hartz, K. E.: Secondary organic aerosol from limona ketone: insights into terpene ozonolysis via synthesis of key intermediates, Phys Chem Chem Phys, 9, 2991-2998, https://doi.org/10.1039/b701333g, 2007.

Draper, D. C., Myllys, N., Hyttinen, N., Møller, K. H., Kjaergaard, H. G., Fry, J. L., Smith, J. N., and Kurtén, T.: Formation of Highly Oxidized Molecules from NO_3 Radical Initiated Oxidation of Δ-3-Carene: A Mechanistic Study, ACS Earth Space Chem., 3, 1460-1470, https://doi.org/10.1021/acsearthspacechem.9b00143, 2019.

Ehn, M., Thornton, J. A., Kleist, E., Sipila, M., Junninen, H., Pullinen, I., Springer, M., Rubach, F., Tillmann, R., Lee, B., Lopez-Hilfiker, F., Andres, S., Acir, I. H., Rissanen, M., Jokinen, T., Schobesberger, S., Kangasluoma, J., Kontkanen, J., Nieminen, T., Kurten, T., Nielsen, L. B., Jorgensen, S., Kjaergaard, H. G., Canagaratna, M., Maso, M. D., Berndt, T., Petaja, T., Wahner, A., Kerminen, V. M., Kulmala, M., Worsnop, D. R., Wildt, J., and Mentel, T. F.: A Large Source of Low-Volatility Secondary Organic Aerosol, Nature, 506, 476-479, https://doi.org/10.1038/nature13032, 2014.

Fan, W., Chen, T., Zhu, Z., Zhang, H., Qiu, Y., and Yin, D.: A review of secondary organic aerosols formation focusing on organosulfates and organic nitrates, J. Hazard. Mater., 430, 128406, https://doi.org/10.1016/j.jhazmat.2022.128406, 2022.

Farmer, D. K., Matsunaga, A., Docherty, K. S., Surratt, J. D., Seinfeld, J. H., Ziemann, P. J., and Jimenez, J. L.: Response of an Aerosol Mass Spectrometer to Organonitrates and Organosulfates and Implications for Atmospheric Chemistry, Proc. Natl. Acad. Sci. U.S.A, 107, 6670-6675, https://doi.org/10.1073/pnas.0912340107, 2010.

Fisher, J. A., Jacob, D. J., Travis, K. R., Kim, P. S., Marais, E. A., Miller, C. C., Yu, K., Zhu, L., Yantosca, R. M., Sulprizio, M. P., Mao, J., Wennberg, P. O., Crounse, J. D., Teng, A. P., Nguyen, T. B., St Clair, J. M., Cohen, R. C., Romer, P., Nault, B. A., Wooldridge, P. J., Jimenez, J. L., Campuzano-Jost, P., Day, D. A., Hu, W., Shepson, P. B., Xiong, F., Blake, D. R., Goldstein, A. H., Misztal, P. K., Hanisco, T. F., Wolfe, G. M., Ryerson, T. B., Wisthaler, A., and Mikoviny, T.: Organic Nitrate Chemistry and Its Implications for Nitrogen Budgets in An Isoprene- and Monoterpene-Rich Atmosphere: Constraints from Aircraft (SEAC^{4}RS) and Ground-Based (SOAS) Observations in the Southeast US, Atmos. Chem. Phys., 16, 5969-5991, https://doi.org/10.5194/acp-16-5969-2016, 2016.

Fry, J. L., Draper, D. C., Barsanti, K. C., Smith, J. N., Ortega, J., Winkler, P. M., Lawler, M. J., Brown, S. S., Edwards, P. M., Cohen, R. C., and Lee, L.: Secondary Organic Aerosol Formation and Organic Nitrate Yield from NO_3 Oxidation of Biogenic Hydrocarbons, Environ. Sci. Technol., 48, 11944-11953, https://doi.org/10.1021/es502204x, 2014.

Fry, J. L., Kiendler-Scharr, A., Rollins, A. W., Brauers, T., Brown, S. S., Dorn, H. P., Dubé, W. P., Fuchs, H., Mensah, A., Rohrer, F., Tillmann, R., Wahner, A., Wooldridge, P. J., and Cohen, R. C.: SOA from Limonene: Role of NO_3 in Its Generation and Degradation, Atmos. Chem. Phys., 11, 3879-3894, https://doi.org/10.5194/acp-11-3879-2011, 2011.

Glasius, M. and Goldstein, A. H.: Recent Discoveries and Future Challenges in Atmospheric Organic Chemistry, Environ. Sci. Technol., 50, 2754-2764, https://doi.org/10.1021/acs.est.5b05105, 2016.

Guenther, A. B., Jiang, X., Heald, C. L., Sakulyanontvittaya, T., Duhl, T., Emmons, L. K., and Wang, X.: The Model of Emissions of Gases and Aerosols from Nature version 2.1 (MEGAN2.1): an Extended and Updated Framework for Modeling Biogenic Emissions, Geosci. Model Dev., 5, 1471-1492, https://doi.org/10.5194/gmd-5-1471-2012, 2012.

Guo, F., Bui, A. A. T., Schulze, B. C., Dai, Q., Yoon, S., Shrestha, S., Wallace, H. W., Sanchez, N. P., Alvarez, S., Erickson, M. H., Sheesley, R. J., Usenko, S., Flynn, J., and Griffin, R. J.: Airmass History, Night-Time Particulate Organonitrates, and Meteorology Impact Urban SOA Formation Rate, Atmos. Environ., 322, https://doi.org/10.1016/j.atmosenv.2024.120362, 2024.

Guo, Y., Shen, H., Pullinen, I., Luo, H., Kang, S., Vereecken, L., Fuchs, H., Hallquist, M., Acir, I.-H., Tillmann, R., Rohrer, F., Wildt, J., Kiendler-Scharr, A., Wahner, A., Zhao, D., and Mentel, T. F.: Identification of Highly Oxygenated Organic Molecules and Their Role in Aerosol Formation in the Reaction of Limonene with Nitrate Radical, Atmos. Chem. Phys., 22, 11323-11346, https://doi.org/10.5194/acp-22-11323-2022, 2022.

Hallquist, M., Wängberg, I., Ljungström, E., Barnes, I., and Becker, K.-H.: Aerosol and Product Yields from NO_3 Radical-Initiated Oxidation of Selected Monoterpenes, Environ. Sci. Technol., 33, 553-559, https://doi.org/10.1021/es980292s, 1999.

Ham, J. E., Harrison, J. C., Jackson, S. R., and Wells, J. R.: Limonene ozonolysis in the presence of nitric oxide: Gas-phase reaction products and yields, Atmos Environ (1994), 132, 300-308, https://doi.org/10.1016/j.atmosenv.2016.03.003, 2016.

Jokinen, T., Berndt, T., Makkonen, R., Kerminen, V. M., Junninen, H., Paasonen, P., Stratmann, F., Herrmann, H., Guenther, A. B., Worsnop, D. R., Kulmala, M., Ehn, M., and Sipila, M.: Production of Extremely Low Volatile Organic Compounds from Biogenic Emissions: Measured Yields and Atmospheric Implications, Proc. Natl. Acad. Sci. U.S.A, 112, 7123-7128, https://doi.org/10.1073/pnas.1423977112, 2015.

Kiendler‐Scharr, A., Mensah, A. A., Friese, E., Topping, D., Nemitz, E., Prevot, A. S. H., Äijälä, M., Allan, J., Canonaco, F., Canagaratna, M., Carbone, S., Crippa, M., Dall Osto, M., Day, D. A., De Carlo, P., Di Marco, C. F., Elbern, H., Eriksson, A., Freney, E., Hao, L., Herrmann, H., Hildebrandt, L., Hillamo, R., Jimenez, J. L., Laaksonen, A., McFiggans, G., Mohr, C., O'Dowd, C., Otjes, R., Ovadnevaite, J., Pandis, S. N., Poulain, L., Schlag, P., Sellegri, K., Swietlicki, E., Tiitta, P., Vermeulen, A., Wahner, A., Worsnop, D., and Wu, H. C.: Ubiquity of Organic Nitrates from Nighttime Chemistry in the European Submicron Aerosol, Geophys. Res. Lett., 43, 7735-7744, https://doi.org/10.1002/2016gl069239, 2016.

Kilgour, D. B., Jernigan, C. M., Zhou, S., Brito de Azevedo, E., Wang, J., Zawadowicz, M. A., and Bertram, T. H.: Contribution of Speciated Monoterpenes to Secondary Aerosol in the Eastern North Atlantic, ACS Environ. Sci. Technol. Air, 555-566, https://doi.org/10.1021/acsestair.3c00112, 2024.

Kurten, T., Moller, K. H., Nguyen, T. B., Schwantes, R. H., Misztal, P. K., Su, L., Wennberg, P. O., Fry, J. L., and Kjaergaard, H. G.: Alkoxy Radical Bond Scissions Explain the Anomalously Low Secondary Organic Aerosol and Organonitrate Yields From alpha-Pinene + NO_3, J. Phys. Chem. Lett., 8, 2826-2834, https://doi.org/10.1021/acs.jpclett.7b01038, 2017.

Kwan, A. J., Chan, A. W. H., Ng, N. L., Kjaergaard, H. G., Seinfeld, J. H., and Wennberg, P. O.: Peroxy Radical Chemistry and OH Radical Production during the NO_3-Initiated Oxidation of Isoprene, Atmos. Chem. Phys., 12, 7499-7515, https://doi.org/10.5194/acp-12-7499-2012, 2012.

Lelieveld, J., Evans, J. S., Fnais, M., Giannadaki, D., and Pozzer, A.: The contribution of outdoor air pollution sources to premature mortality on a global scale, Nature, 525, 367-371, https://doi.org/10.1038/nature15371, 2015.

Li, Y., Fu, T. M., Yu, J. Z., Yu, X., Chen, Q., Miao, R., Zhou, Y., Zhang, A., Ye, J., Yang, X., Tao, S., Liu, H., and Yao, W.: Dissecting the Contributions of Organic Nitrogen Aerosols to Global Atmospheric Nitrogen Deposition and Implications for Ecosystems, Natl. Sci. Rev., https://doi.org/10.1093/nsr/nwad244, 2023a.

Li, Y., Fu, T. M., Yu, J. Z., Yu, X., Chen, Q., Miao, R., Zhou, Y., Zhang, A., Ye, J., Yang, X., Tao, S., Liu, H., and Yao, W.: Dissecting the contributions of organic nitrogen aerosols to global atmospheric nitrogen deposition and implications for ecosystems, Natl. Sci. Rev., 10, 244, https://doi.org/10.1093/nsr/nwad244, 2023b.

Lin, G., Sillman, S., Penner, J. E., and Ito, A.: Global modeling of SOA: the use of different mechanisms for aqueous-phase formation, Atmos. Chem. Phys., 14, 5451-5475, https://doi.org/10.5194/acp-14-5451-2014, 2014.

Liu, D., Zhang, Y., Zhong, S., Chen, S., Xie, Q., Zhang, D., Zhang, Q., Hu, W., Deng, J., Wu, L., Ma,

C., Tong, H., and Fu, P.: Large Differences of Highly Oxygenated Organic Molecules (HOMs) and Low-Volatile Species in Secondary Organic Aerosols (SOAs) Formed from Ozonolysis of β-pinene and Limonene, Atmos. Chem. Phys., 23, 8383-8402, https://doi.org/10.5194/acp-23-8383-2023, 2023.

Luo, H., Vereecken, L., Shen, H., Kang, S., Pullinen, I., Hallquist, M., Fuchs, H., Wahner, A., Kiendler-Scharr, A., Mentel, T. F., and Zhao, D.: Formation of Highly Oxygenated Organic Molecules from the Oxidation of Limonene by OH Radical: Significant Contribution of H-abstraction Pathway, Atmos. Chem. Phys., 23, 7297-7319, https://doi.org/10.5194/acp-23-7297-2023, 2023.

Matsunaga, A. and Ziemann, P. J.: Branching Ratios and Rate Constants for Decomposition and Isomerization of beta-Hydroxyalkoxy Radicals Formed from OH Radical-Initiated Reactions of C_6-C_{13} 2-Methyl-1-Alkenes in the Presence of NO_x, J Phys Chem A, 123, 7839-7846, https://doi.org/10.1021/acs.jpca.9b06218, 2019.

Mayhew, A. W., Edwards, P. M., and Hamilton, J. F.: Daytime isoprene nitrates under changing NOx and O3, Atmos. Chem. Phys., 23, 8473-8485, https://doi.org/10.5194/acp-23-8473-2023, 2023.

Mayorga, R., Xia, Y., Zhao, Z., Long, B., and Zhang, H.: Peroxy Radical Autoxidation and Sequential Oxidation in Organic Nitrate Formation during Limonene Nighttime Oxidation, Environ. Sci. Technol., 15337-15346, https://doi.org/10.1021/acs.est.2c04030, 2022.

McFiggans, G., Mentel, T. F., Wildt, J., Pullinen, I., Kang, S., Kleist, E., Schmitt, S., Springer, M., Tillmann, R., Wu, C., Zhao, D., Hallquist, M., Faxon, C., Le Breton, M., Hallquist, A. M., Simpson, D., Bergstrom, R., Jenkin, M. E., Ehn, M., Thornton, J. A., Alfarra, M. R., Bannan, T. J., Percival, C. J., Priestley, M., Topping, D., and Kiendler-Scharr, A.: Secondary organic aerosol reduced by mixture of atmospheric vapours, Nature, 565, 587-593, https://doi.org/10.1038/s41586-018-0871-y, 2019.

Moldanova, J. and Ljungström, E.: Modelling of Particle Formation from NO_3 Oxidation of Selected Monoterpenes, J. Aerosol Sci., 31, 1317-1333, https://doi.org/10.1016/S0021-8502(00)00041-0, 2000.

Ng, N. L., Brown, S. S., Archibald, A. T., Atlas, E., Cohen, R. C., Crowley, J. N., Day, D. A., Donahue, N. M., Fry, J. L., Fuchs, H., Griffin, R. J., Guzman, M. I., Herrmann, H., Hodzic, A., Iinuma, Y., Jimenez, J. L., Kiendler-Scharr, A., Lee, B. H., Luecken, D. J., Mao, J., McLaren, R., Mutzel, A., Osthoff, H. D., Ouyang, B., Picquet-Varrault, B., Platt, U., Pye, H. O. T., Rudich, Y., Schwantes, R. H., Shiraiwa, M., Stutz, J., Thornton, J. A., Tilgner, A., Williams, B. J., and Zaveri, R. A.: Nitrate Radicals and Biogenic Volatile Organic Compounds: Oxidation, Mechanisms, and Organic Aerosol, Atmos. Chem. Phys., 17, 2103-2162, https://doi.org/10.5194/acp-17-2103-2017, 2017.

Pankow, J. F. and Asher, W. E.: SIMPOL.1: a simple group contribution method for predicting vapor pressures and enthalpies of vaporization of multifunctional organic compounds, Atmos. Chem. Phys., 8, 2773-2796, https://doi.org/10.5194/acp-8-2773-2008, 2008.

Perring, A. E., Pusede, S. E., and Cohen, R. C.: An Observational Perspective on the Atmospheric Impacts of Alkyl and Multifunctional Nitrates on Ozone and Secondary Organic Aerosol, Chem. Rev., 113, 5848-5870, https://doi.org/10.1021/cr300520x, 2013.

Picquet-Varrault, B., Suarez-Bertoa, R., Duncianu, M., Cazaunau, M., Pangui, E., David, M., and Doussin, J.-F.: Photolysis and oxidation by OH radicals of two carbonyl nitrates: 4-nitrooxy-2-butanone and 5-nitrooxy-2-pentanone, Atmos. Chem. Phys., 20, 487-498, https://doi.org/10.5194/acp-20-487-2020, 2020.

Pye, H. O., Luecken, D. J., Xu, L., Boyd, C. M., Ng, N. L., Baker, K. R., Ayres, B. R., Bash, J. O., Baumann, K., Carter, W. P., Edgerton, E., Fry, J. L., Hutzell, W. T., Schwede, D. B., and Shepson, P. B.: Modeling the Current and Future Roles of Particulate Organic Nitrates in the Southeastern United States, Environ. Sci. Technol., 49, 14195-14203, https://doi.org/10.1021/acs.est.5b03738, 2015.

Rollins, A. W., Kiendler-Scharr, A., Fry, J. L., Brauers, T., Brown, S. S., Dorn, H. P., Dubé, W. P., Fuchs, H., Mensah, A., Mentel, T. F., Rohrer, F., Tillmann, R., Wegener, R., Wooldridge, P. J., and Cohen, R. C.: Isoprene Oxidation by Nitrate Radical: Alkyl Nitrate and Secondary Organic Aerosol Yields, Atmos. Chem. Phys., 9, 6685-6703, https://doi.org/10.5194/acp-9-6685-2009, 2009.

Sato, K., Inomata, S., Xing, J.-H., Imamura, T., Uchida, R., Fukuda, S., Nakagawa, K., Hirokawa, J., Okumura, M., and Tohno, S.: Effect of OH Radical Scavengers on Secondary Organic Aerosol Formation from Reactions of Isoprene with Ozone, Atmos. Environ., 79, 147-154, https://doi.org/10.1016/j.atmosenv.2013.06.036, 2013.

Shen, C., Yang, X., Thornton, J., Shilling, J., Bi, C., Isaacman-VanWertz, G., and Zhang, H.: Observation-constrained kinetic modeling of isoprene SOA formation in the atmosphere, Atmos. Chem. Phys., 24, 6153-6175, https://doi.org/10.5194/acp-24-6153-2024, 2024.

Shen, H., Zhao, D., Pullinen, I., Kang, S., Vereecken, L., Fuchs, H., Acir, I. H., Tillmann, R., Rohrer, F., Wildt, J., Kiendler-Scharr, A., Wahner, A., and Mentel, T. F.: Highly Oxygenated Organic Nitrates Formed from NO_3 Radical-Initiated Oxidation of beta-Pinene, Environ. Sci. Technol., 55, 15658-15671, https://doi.org/10.1021/acs.est.1c03978, 2021.

Sindelarova, K., Granier, C., Bouarar, I., Guenther, A., Tilmes, S., Stavrakou, T., Müller, J. F., Kuhn, U., Stefani, P., and Knorr, W.: Global Data Set of Biogenic VOC Emissions Calculated by the MEGAN Model over the last 30 years, Atmos. Chem. Phys., 14, 9317-9341, https://doi.org/10.5194/acp-14-9317-2014, 2014.

Spittler, M., Barnes, I., Bejan, I., Brockmann, K. J., Benter, T., and Wirtz, K.: Reactions of NO_3 Radicals with Limonene and α-pinene: Product and SOA Formation, Atmos. Environ., 40, 116-127, https://doi.org/10.1016/j.atmosenv.2005.09.093, 2006.

Surratt, J. D., Gómez-González, Y., Chan, A. W. H., Reinhilde, V., Mona, S., E, K. T., O, E. E., H, O. J., Michael, L., Mohammed, J., Willy, M., Magda, C., C, F. R., and H, S. J.: Organosulfate Formation in Biogenic Secondary Organic Aerosol, J. Phys. Chem. A, 112, https://doi.org/10.1021/jp802310p, 2008.

Tao, J., Zhang, L., Cao, J., and Zhang, R.: A review of current knowledge concerning $PM_{2.5}$ chemical composition, aerosol optical properties and their relationships across China, Atmos. Chem. Phys., 17, 9485-9518, https://doi.org/10.5194/acp-17-9485-2017, 2017.

Wang, Y., Takeuchi, M., Wang, S., Nizkorodov, S. A., France, S., Eris, G., and Ng, N. L.: Photolysis of Gas-Phase Atmospherically Relevant Monoterpene-Derived Organic Nitrates, J Phys Chem A, 127, 987-999, https://doi.org/10.1021/acs.jpca.2c04307, 2023.

Xu, L., Tsona, N. T., You, B., Zhang, Y., Wang, S., Yang, Z., Xue, L., and Du, L.: NO_x Enhances Secondary Organic Aerosol Formation from Nighttime γ-terpinene Ozonolysis, Atmos. Environ., 225, https://doi.org/10.1016/j.atmosenv.2020.117375, 2020.

Yu, K., Zhu, Q., Du, K., and Huang, X.-F.: Characterization of Nighttime Formation of Particulate Organic Nitrates Based on High-Resolution Aerosol Mass Spectrometry in an Urban Atmosphere in China, Atmos. Chem. Phys., 19, 5235-5249, https://doi.org/10.5194/acp-19-5235-2019, 2019.

Zang, H., Luo, Z., Li, C., Li, Z., Huang, D., and Zhao, Y.: Nocturnal Atmospheric Synergistic Oxidation Reduces the Formation of Low-Volatility Organic Compounds from Biogenic Emissions, Atmos. Chem. Phys., 24, 11701-11716, https://doi.org/10.5194/acp-24-11701-2024, 2024.

Zare, A., Fahey, K. M., Sarwar, G., Cohen, R. C., and Pye, H. O. T.: Vapor-Pressure Pathways Initiate but Hydrolysis Products Dominate the Aerosol Estimated from Organic Nitrates, ACS Earth Space Chem., 3, 1426-1437, https://doi.org/10.1021/acsearthspacechem.9b00067, 2019.

Zhao, D. F., Kaminski, M., Schlag, P., Fuchs, H., Acir, I. H., Bohn, B., Häseler, R., Kiendler-Scharr, A.,

Rohrer, F., Tillmann, R., Wang, M. J., Wegener, R., Wildt, J., Wahner, A., and Mentel, T. F.: Secondary Organic Aerosol Formation from Hydroxyl Radical Oxidation and Ozonolysis of Monoterpenes, Atmos. Chem. Phys., 15, 991-1012, https://doi.org/10.5194/acp-15-991-2015, 2015.